analytical chemistry

Article

pubs.acs.org/ac

Target-Specific Imaging of Transmembrane Receptors Using Quinonyl Glycosides Functionalized Quantum Dots

Wei Ma,[†] Hui-Ting Liu,[†] Xiao-Peng He,*[,†] Yi Zang,[‡] Jia Li,*[,‡] Guo-Rong Chen,[†] He Tian,[†] and Yi-Tao Long*[,†]

[†]Key Laboratory for Advanced Materials & Institute of Fine Chemicals, East China University of Science and Technology, Shanghai, P. R. China

[‡]National Center for Drug Screening, State Key Laboratory of Drug Research, Shanghai Institute of Materia Medica, Shanghai Institutes of Biological Sciences, Chinese Academy of Sciences, Shanghai, P. R. China

Supporting Information

ABSTRACT: Here, we describe a novel "switch-on" biosensor based on quinonyl glycosides functionalized quantum dots (QDs) for the specific targeting and imaging of transmembrane glycoprotein receptors on the surface of cancer cells. The design of the quinonyl glycosides lies in that the quinone moiety serves as a quencher of QDs and the glycoside moiety as a biospecific ligand for targeting a receptor. We observed that the quenched photoluminescence of the quinone glycosides functionalized QDs could be significantly recovered by a specific lectin that selectively binds to the glycosides clustering the QDs but was not affected by a panel of nonspecific lectins. Moreover, we determined that quinonyl galactoside functionalized QDs could optically image the asialoglycoprotein receptors of a hepatoma cell line in a target-specific manner. This system might provide new insights into the fabrication of photoluminogenic biosensors for the analysis of the universal ligand−receptor recognitions in nature.

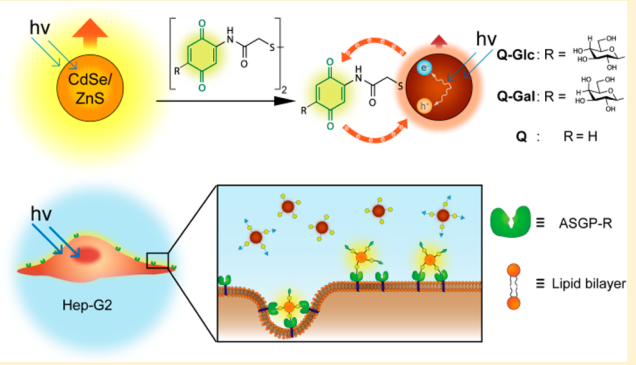

Sensory transmembrane proteins, such as the G protein-coupled receptors, can recognize a plethora of endogenous and exogenous ligands and stimuli, leading to activation of downstream cellular signal pathways.[1] These natural "lock and key" interactions universally found in eukaryotes, such as those between the sugar ligands and their receptors, are crucial for a number of biological and pathological events including cell−cell adhesion, cell development and differentiation, virus invasion, and cancer metastasis.[2−6] Therefore, the clear interpretation of these vital bioevents may facilitate our understanding toward life science. In the meanwhile, biosensors or drug delivery systems anchored with ligand molecules that target specific receptors uniquely expressed on the surface of malignant cells have been developed, which results in improved disease theranostics.[7−13]

Semiconductor quantum dots (QDs), a class of unique nanocrystals, possess attractive optical properties such as tunable photoluminescence (PL), narrow emission, broad absorption profiles, high signal brightness, and superior photostability as compared to organic dyes.[14] In addition, QDs have been employed in widespread areas ranging from *in vivo* imaging to clinical diagnostics due to their ultrasensitivity toward charge transfer. Therefore, judicious control of the electron/charge transfer of QDs functionalized with redox centers has been of increasing interest in the development of biosensors.[15−19] Quinones are inarguably the most prevailing electroactive species used to modify QDs, where quinone acts as an effective electron acceptor to quench the PL of QDs. Whereas current studies mainly focus on the employment of quinonyl QDs to investigate redox-based regulation of signal transduction,[16−19] we exemplify here a novel strategy that uses QDs functionalized with quinonyl glycoside ligands for the target-specific, photoluminogenic (that generates PL) imaging of transmembrane receptors expressed by cancer cells (Figure 1).

EXPERIMENTAL SECTION

Electrochemistry. A two-compartment glass cell equipped with a cation-exchange membrane was used for electrochemical measurements. Anodic solution was stirred by a magnetic stir bar, and the anode zone was equipped with a gas inlet and outlet. Ag/AgCl was used as the reference electrode and glassy carbon foils as the working electrode with a distance between the cathode and anode of ~7.5 cm. Platinum was used as the cathode. Electrochemical oxidation of the 1,4-dimethoxybenzene, *C*-glucosyl-1,4-dimethoxybenzene, and *C*-galactosyl-1,4-

Received: February 25, 2014
Accepted: May 7, 2014
Published: May 7, 2014

   dx.doi.org/10.1021/ac501463u | *Anal. Chem.* 2014, 86, 5502−5507

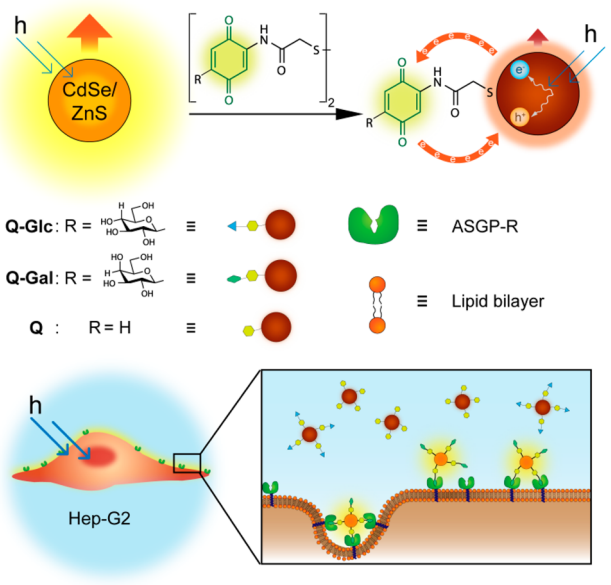

Figure 1. Schematic diagram of quinonyl glycosides functionalized QDs as a "switch-on" PL biosensor for target-specific imaging of ASGP-R on Hep-G2 cancer cells (**Q-Glc**, quinonyl glucoside disulfide; **Q-Gal**, quinonyl galactoside disulfide; **Q**, quinonyl disulfide; ASGP-R, asialoglycoprotein receptor).

dimethoxybenzene were carried out at a glassy carbon foils electrode in CH_3CN containing 0.15 M Bu_4NBF_4 in the presence of a large excess of H_2O (~1 M). For all electrochemical experiments, oxygen was removed by bubbling N_2 through the solution prior to measurements. Experiments were generally stopped when the passed charge reached that theoretically required for the total conversion of the substrate with a two-electron process. Different values of the working potential were tested.

Preparation of Functionalized CdSe/ZnS QDs. CdSe/ZnS QDs (5 μM) were incubated with benzoquinonyl-*C*-glucoside-tailed disulfides (**Q-Glc**), benzoquinonyl-*C*-galactoside-tailed disulfides (**Q-Gal**), benzoquinone-tailed disulfides (**Q**), and sulfhydryl aryl *C*-galactose (**Ph-Gal**) of different concentrations in 0.2 M phosphate buffer saline (PBS, pH 7.4) and then shaken vigorously for 30 min in order to coat these ligands onto the QDs.[16,18,20−24] Then acetone was added with a volume ratio of 1:1 to the mixture which was centrifuged at 7840 rpm for 20 min to remove any nonspecific aggregates, resulting in pellets of supernatant CdSe/ZnS nanocrystals which were purified three times.

High-Performance Size Exclusion Chromatography Measurement. Size exclusion chromatography using a hydroxylated polymethacrylate-based gel and Agilent high-performance liquid chromatograph (1100 series) equipped with a differential refractive index detectors. A mobile phase of 10 mM PBS buffer (pH = 7.4) was delivered at a flow rate of 0.6 mL/min over a TSK $PW_{XL}G3000$ SEC column. Samples were dissolved in PBS buffer to a concentration of ~1 mg/mL, and injection volumes were 20 μL.

Hydrodynamic Diameter Measurements by Dynamic Light Scattering. Light scattering analysis was performed with a Zetasizer Nano-ZS Instrument (ZEM4228) from Malvern Instruments using the protocols provided by the supplier. The concentration of CdSe/ZnS QDs and **Q-Gal** functionalized CdSe/ZnS QDs was 2−3 mM, and all samples were filtered through a 200 μm filter before analysis.

Cell Culture, Cellular Imaging, and Cytotoxicity. Hep-G2 cells were cultured in a Dulbecco's Modified Eagle's Medium (Invitrogen, Carlsbad, CA) supplemented with a 10% Fetal bovine serum (Gibco, Gland Island, NY) at 37 °C in a 5% humidified CO_2 air environment. The functionalized QD bioconjugates were added to the culture medium, which was then incubated for 2 h. Then the growth medium was removed, and the cells were fixed with 4% methanal solution at room temperature for 20 min, followed by washing with PBS three times. A cover glass was then mounted on a microscopic glass slide, and the imaging behavior was studied under a microscope. The images were taken by using an inverted PL scanning microscope with an objective lens (60×). All background parameters (the laser intensity, exposure time, and objective lens) were kept constant when the different PL images were captured. The cytotoxicity assays were performed by the 3-(4,5-dimethylthiazol-2-yl)-2,5-diphenyltetrazolium bromide (MTT) assay. Hep-G2 cells were placed in 96-well culture plates (10^4 cells/well) and allowed to attach for 24 h before treatment. The cells were treated with CdSe/ZnS QDs capped with the **Q-Gal**. The cell viability was evaluated by the MTT assay for Hep-G2 cells after 24 h treatment.

Silencing of ASGP-R1 Gene by RNA Interference. Silencing of the ASGP-R1 gene expression on Hep-G2 cells was mediated by an ASGPR-1 gene-specific or a scrambled (control) siRNA oligonucleotide duplex purchased from Santa Cruz Biotechnologies (Santa Cruz, CA). Briefly, Hep-G2 cells were seeded at 4×10^5 cells/well in a 6-well plate, and lipofectamine 2000 (Invitrogen) was used for transfection as instructed by the manufacturer. After incubating the cells with siRNA for 6 h, the lipofetamine-siRNA-complex containing medium was replaced. After another 48 h, the cells were harvested for experiments and the level of ASGP-R1 mRNA was evaluated by quantitative real-time PCR.

Detection of ASGP-R1 mRNA by Quantitative Real-Time RT-PCR. Total cellular RNAs were extracted from Hep-G2 cells using TRIzol Reagent (Invitrogen) according to the manufacturer's instructions. mRNA was reversely transcribed using the SuperScript First-Strand Synthesis System (TAKARA). For quantitative PCR reactions, 1:10 dilutions of cDNA products were amplified using SYBR Green PCR Master Mix (TAKARA) and analyzed by using ABI Prism 7300 Fast system (Applied Biosystems). All samples were run in triplicate in each experiment. The specificity of detected signals was confirmed by a dissociation curve consisting of a single peak. Values were normalized on the basis of GAPDH m RNA. The forward (fp) and reverse (rp) primers for the reactions were as follows:

ASGP-R1-fp	5′-CTGGACAATGAGGAGAGTGAC-3′
ASGP-R1-rp	5′-TTGAAGCCCGTCTCGTAGTC-3′
GAPDH-fp	5′-ATCACTGCCACCCAGAAGAC-3′
GAPDH-rp	5′-ATGAGGTCCACCACCCTGTT-3′

RESULTS AND DISCUSSION

Design and Fabrication of Quinonyl Glycosides Functionalized QDs. We have demonstrated in a previous study that an electrochemical deprotection/oxidation strategy offers a practical route to obtaining sulfhydryl benzoquinonyl *C*-glycosides from sulfhydryl aryl *C*-glycosides confined on a gold surface.[25] Continuing these efforts, in this work we further employed the tactic to acquire the desired quinonyl glycosides

dx.doi.org/10.1021/ac501463u | *Anal. Chem.* 2014, 86, 5502−5507

at a carbon electrode (Supporting Information, Figure S1).[26−28] As shown in Figure 1, we established a model system for the target-specific recognition, in which CdSe/ZnS QDs are functionalized with quinonyl *C*-glycoside-tailed disulfides (**Q-Glc** or **Q-Gal**), quinone-tailed disulfide (**Q**) and sulfhydryl dimethoxybenzene *C*-galactoside (**Ph-Gal**) were used as negative controls. The designed quinonyl glycosides are envisioned to have dual functions: the quinone moiety of the system serves as a quencher of the QDs and the glycoside moiety as a biospecific ligand for targeting the receptors. Moreover, the clustering manner of quinonyl glycosides on the QD surface highly mimics the topology of the cell-surface glycans, leading to enhanced binding avidity (amplified signal) with the receptors, thus overcoming the low binding affinity between a sugar and a receptor protein.[29]

To characterize the quinonyl glycosides functionalized QDs, the **Q-Gal** QDs were selected as a model. Upon coating with **Q-Gal**, the PL of QDs quenched significantly, whereas the UV−vis spectrum of which did not change markedly (Figure 2a). The data elicited from PL spectroscopy suggests that the quinonyl compounds could quench the PL of QDs.[30] Transmission electron microscopy (TEM) imaging showed that the **Q-Gal** QDs (Figure 2c) were monodisperse particles of the same highly crystalline form as the unmodified CdSe/ZnS QDs (Figure 2b). To investigate the particle size enlargement of the functionalized QDs, a dynamic light scattering (DLS) experiment was performed using bare QDs and **Q-Gal** QDs (Figure 2d). DLS of the bare CdSe/ZnS QDs in aqueous solution reveals that the QDs have a narrow size distribution with an average size of 3.6 nm (Figure 2d, black line), whereas the **Q-Gal** functionalized CdSe/ZnS QD bioconjugates became slightly larger with an average size of 3.8 nm (Figure 2d, red line), consistent with the coating of disulfide compounds onto the surface of the QDs.[31] Moreover, high-performance liquid chromatography was performed on a 30 cm long size exclusion column (SEC). Representative SEC results show the retention time decrease of **Q-Gal** functionalized CdSe/ZnS QD bioconjugates (Figure 2e, red line) compared with bare CdSe/ZnS QDs (Figure 2e, black line). The larger particles (**Q-Gal** functionalized QDs) elute first as expected for a size exclusion process, indicating that quinonyl glycosides disulfide could stably coat the surface of CdSe/ZnS QDs.

PL Spectroscopy of Quinonyl Glycosides Functionalized CdSe/ZnS QDs. To test the effect of the compound-to-QD ratio on the PL quenching of the functionalized QDs, increasing **Q-Glc**, **Q-Gal**, **Q**, or **Ph-Gal** was functionalized onto the CdSe/ZnS QDs. A characteristic decrease in PL intensity was observed for the quinonyl glycosides functionalized QDs (Figure 3a−c), compared with the unconjugated CdSe/ZnS QDs. PL quenching of QD bioconjugates likely arose from the electron-transfer process from the photoexcited QDs to the attached electron-deficient quinone moiety.[16] Following photoexcitation, the conduction-band electron of QDs is transferred to the lowest unoccupied molecular orbital of quinone acceptor, and the electron is then shuttled back to the valence band of QD through nonradiative pathways (Figure 3e). Thus, quinones exhibit surface-related trap states that undergo fast nonradiative de-excitation routes for photoinduced electron carriers, leading to PL quenching.[17,30]

The intensity of the PL emission peak of the QD bioconjugates decreased with increasing ratios (10−50) of **Q-Glc** and **Q-Gal** attached to the QDs, while further increase of ligand molecules did not lead to PL quenching. Similarly, maximum PL quenching of **Q** QDs was reached with an average ratio of 60 quinone molecules per QD. The insets of Figure 3a−c schematically depict the linear PL quenching response of QD bioconjugates as a function of increasing

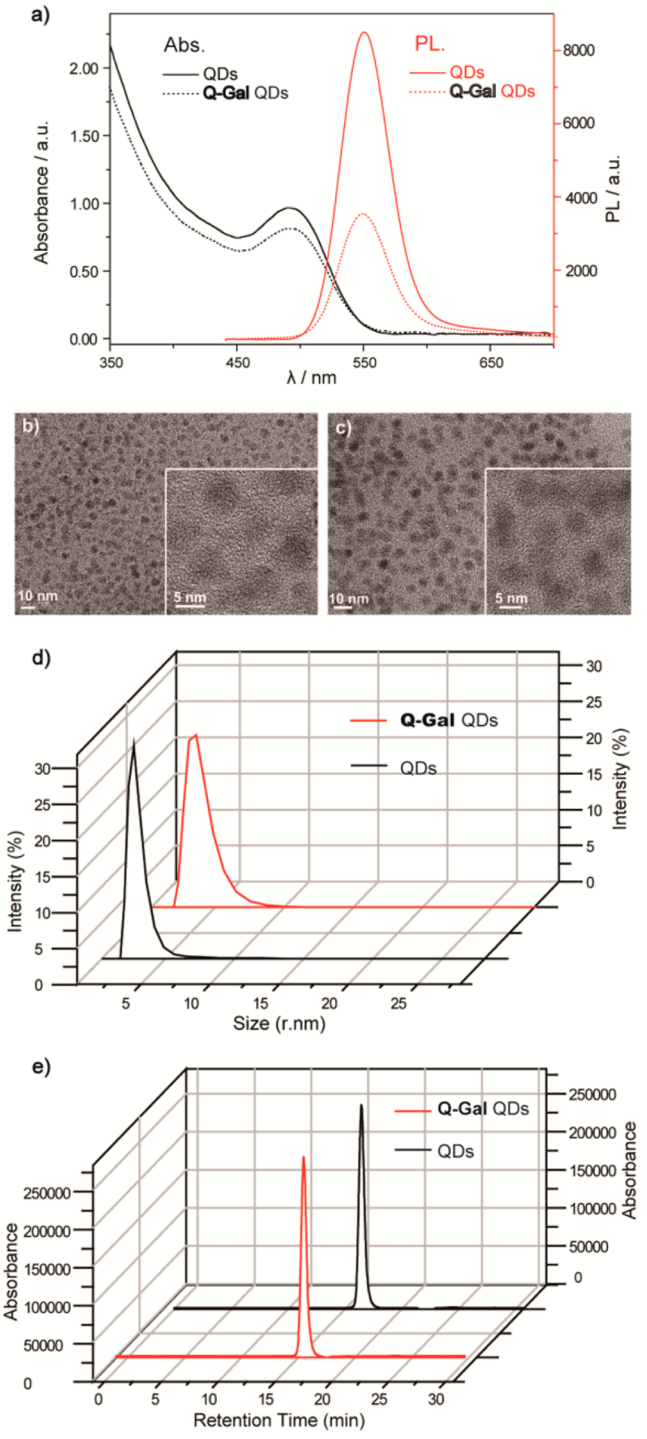

Figure 2. Characterization of **Q-Gal** QDs. (a) Representative PL spectra (red) and UV−vis spectra (black) of bare CdSe/ZnS QDs (straight lines) and **Q-Gal** QDs (dotted lines) in a PBS buffer. (b) TEM image of bare CdSe/ZnS QDs. Inset: a magnified area. (c) TEM image of **Q-Gal** QDs. Inset: a magnified area. (d) DLS measurements of the hydrodynamic radius of bare CdSe/ZnS QDs (black line) and **Q-Gal** functionalized CdSe/ZnS QDs (red line) at room temperature. (e) Representative SEC of bare CdSe/ZnS QDs (black line) and **Q-Gal** functionalized CdSe/ZnS QDs (red line).

dx.doi.org/10.1021/ac501463u | *Anal. Chem.* 2014, 86, 5502−5507

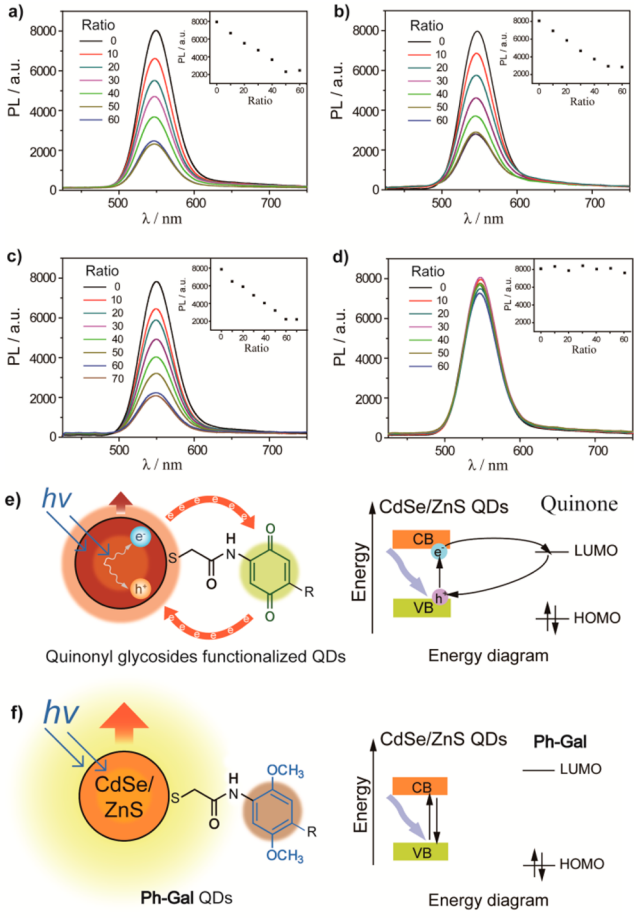

Figure 3. Effect of quinonyl glycosides on PL variation of QDs. Representative PL spectra collected from CdSe/ZnS QDs recorded before and after functionalization with an increasing ratio of (a) **Q-Glc**, (b) **Q-Gal**, (c) **Q**, and (d) **Ph-Gal**. Inset: plotting of PL at 550 nm versus the **Q-Glc**, **Q-Gal**, **Q**, and **Ph-Gal** to CdSe/ZnS QDs ratio. Mechanism of PL changing and energy diagram of (e) quinonyl glycosides (**Q-Glc**, **Q-Gal**, **Q**) functionalized QDs, and (f) **Ph-Gal** functionalized QDs.

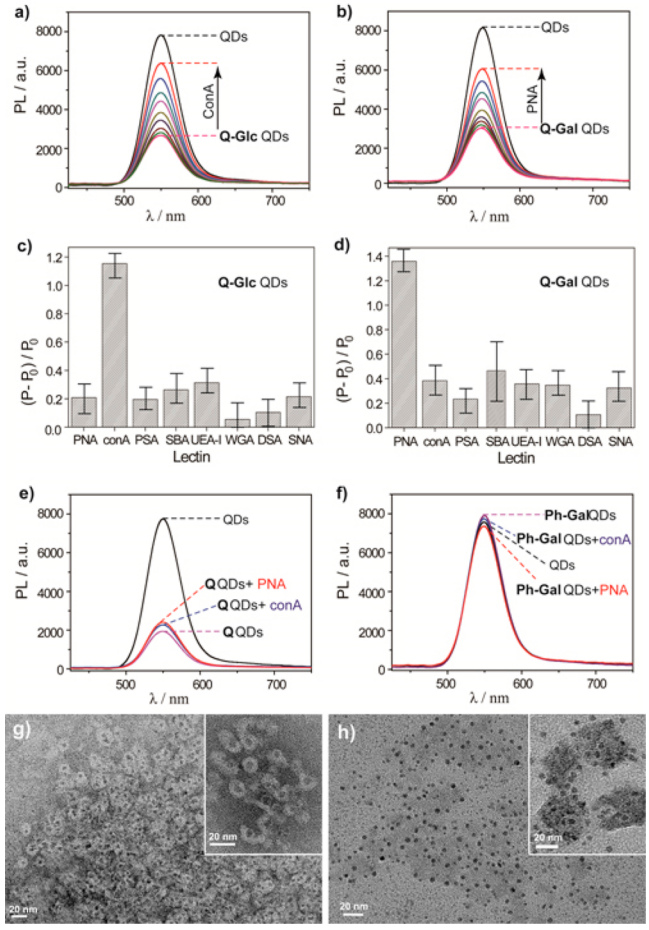

Figure 4. Biospecificity of quinonyl glycosides QDs. The gradual PL recovery of (a) **Q-Glc** QDs and (b) **Q-Gal** QDs upon addition of increasing Con A and PNA ranging from 0.05 to 15 μM, respectively. PL recovery ratio of (c) **Q-Glc** QDs and (d) **Q-Gal** QDs upon addition of 15 μM of various specific or nonspecific lectins (where P_0 is the maximally quenched and P the recovered PL intensity). PL change of (e) **Q** QDs and (f) **Ph-Gal** QDs upon addition of 15 μM of Con A and PNA. TEM image of **Q-Gal** QDs conjugated with (g) the specific lectin PNA (negatively stained with 1% phosphotungstic acid, pH = 7.0) and (h) an unspecific lectin Con A. Inset: a magnified area.

quinones (**Q-Glc**, **Q-Gal**, and **Q**). However, in a control experiment, a **Ph-Gal** QD did not show quenched PL (Figure 3d), because the photoexcited **Ph-Gal** QDs might decay radiatively to the ground state as the **Ph-Gal** is a poor electron acceptor (Figure 3f). This further confirms that the PL quenching was a result of the presence of the quinone moiety on the QD surface.

Detection of Lectins. With the quenching phenomenon observed, we subsequently investigated the PL recoverability of these QD bioconjugates using a range of plant lectins that selectively recognize sugars. Addition of a specific lectin (0.05–15 μM) gradually restored the PL of **Q-Glc** QDs (Concanavalin A, Con A; Figure 4a) and **Q-Gal** QDs (peanut agglutinin, PNA; Figure 4b), and the maximal recovery rate, calculated from $(P - P_0)/P_0$ (where P is the recovered PL intensity of QD bioconjugates by lectin and P_0 is the maximally quenched PL of QD bioconjugates) for **Q-Glc** and **Q-Gal** QDs were determined to be 115% and 135%, respectively. In a previous study, we resolved the cocrystal structure of a hydroquinonyl glucoside with a glycogen phosphorylase and determined that while the glycosyl moiety is swallowed by the sugar-recognition domain of the enzyme, the quinone group is simultaneously bound by a nearby hydrophobic pocket.[32] This has also been viewed as a common feature of lectin–glycoside interactions.[25,32] Thus, we ascribe the PL recovery of the QD bioconjugates to encapsulation of both the glycosyl and quinonyl moieties by the lectin, impairing the electron transfer from QDs to quinone.[16–18]

To further scrutinize the biospecificity of this system, nonspecific lectins that are known to recognize other natural saccharides were tested (Supporting Information, Figure S2). The trivial PL variations of **Q-Glc** QDs (Figure 4c) and **Q-Gal** QDs (Figure 4d) in the presence of a variety of nonspecific lectins, including the *Pisum sativum agglutinin* (PSA, a mannose-specific lectin), *Ulex europeaus* agglutinin (UEA-I, a fucose-specific lectin), wheat germ agglutinin (WGA, a N-acetyl-glucosamine-specific lectin), *Datura stramonium* agglutinin (DSA, a N-acetyl-glucosamine-specific lectin), and *Sambucus nigra* agglutinin (SNA, a sialic acid-specific lectin), reveal the good specificity of the biosensors. We note that the addition of SBA to the **Q-Gal** QDs led to a moderate PL recovery; because besides N-acetyl-galactosamine, this lectin also binds with

dx.doi.org/10.1021/ac501463u | *Anal. Chem.* 2014, 86, 5502–5507

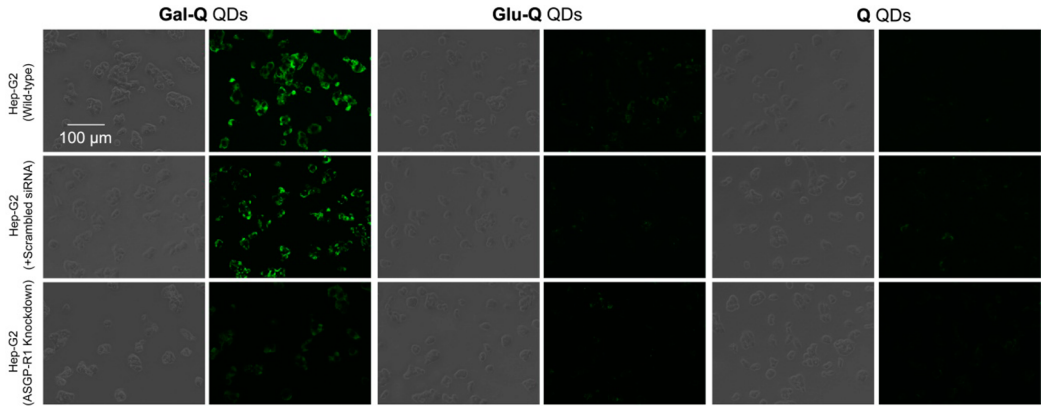

Figure 5. PL imaging of three groups of Hep-G2 cells (wild-type, those treated with scrambled siRNA and ASGP-R1-Knockdown) using quinonyl glycosides functionalized QDs. Bright-field image and PL micrographs collected from wild-type, control (scrambled siRNA), and ASGP-R1 Knockdown Hep-G2 cells with 550 nm-emitting **Q-Glc** functionalized QDs, **Q-Gal** functionalized QDs, and **Q** functionalized QDs.

galactose but with a lower affinity. Moreover, we observed that incubation of 15 μM of Con A or PNA with the **Q** functionalized QDs caused almost no PL recovery (Figure 4e), indicating that QDs functionalized with quinone devoided of a glycosyl precursor is not sensitive to lectins. Likewise, incubation of the lectins with **Ph-Gal** QDs hardly led to any PL signal variation (Figure 4f), which underpins the pivotal role of quinone as PL quencher in this photoluminogenic QD-based biosensor system.

In addition, TEM was employed to evaluate the specific interaction of **Q-Gal** QDs with lectins. **Q-Gal** QDs were coincubated with a specific or a nonspecific lectin in a PBS (pH 7.4) for 30 min and then imaged under a microscope; the encapsulation of **Q-Gal** QDs due to specific binding with PNA was visualized (Figure 4g). Note that a regular arrangement pattern resolved from the TEM image in the case of the unspecific Con A (Figure 4h) might simply be the result of the weak nonspecific adsorption of Con A on the **Q-Gal** QDs. These data positively validate the excellent biospecificity of the established QDs system capped with a quinone quencher covalently linked to an exposed biospecific glycoside.

Imaging of Cell-Surface Receptors. Having demonstrated the effectiveness of QD bioconjugates in sensing sugar-specific lectin producing a "switch-on" PL signal, we further used these sensors for the target-specific imaging of transmembrane receptors. A human hepatoma cell line, Hep-G2, which expresses the asialoglycoprotein receptors (ASGP-R) that recognize galactosyl residues[34] was used for the cellular bioimaging. To ensure that labeling of the cells will be modulated by the sugar-receptor recognitions, knockdown of the ASGP-R1 gene in Hep-G2 was carried out by transfecting the cells with an ASGP-R1 targeting siRNA or a scrambled siRNA ineffective to gene silencing as a control.[35] Quantitative reverse transcription-polymerase chain reaction (RT-PCR) was used to determine the mRNA level of ASGP-R1. Results showed that transfection of Hep-G2 cells with the ASGP-R1 specific siRNA duplex depleted the gene by ~70%, whereas incubation of scrambled siRNA did not interfere with the expression of ASGP-R1 (Supporting Information, Figure S3).[36−38] The Hep-G2 cells for imaging were classified into three groups: the wild-type (unmodified), control (treated with scrambled siRNA), and ASGP-R1-Knockdown (treated with ASGP-R1-specific siRNA) cells.

To confirm the biospecific imaging of Hep-G2 cells via the functionalized QDs, we employed **Q-Glc**, **Q-Gal**, and **Q** QDs for the tests. As shown in Figure 5, bright-field images of all cell groups loaded with the QD bioconjugates first illustrate that cells are viable throughout the experiments. After loading of **Q-Gal** QDs, wild-type Hep-G2 cells displayed a significant PL probably due to the specific galactose-ASGP-R recognition. Similarly, the PL signal of **Q-Gal** QDs was also strongly activated with the control Hep-G2 cells (treated with scrambled siRNA). By contrast, we observed that the PL recovery of **Q-Gal** QDs became much weakened after incubation with ASGP-R1-Knockdown Hep-G2 cells with a reduced ASGP-R1 expression level. This suggests that reducing the receptor level results in a decreased PL recoverability for **Q-Gal** QDs. Furthermore, only faint PL was observed with the cells using **Q-Glc** or **Q** QDs probably due to the lack of a specific binding for Hep-G2 cells.

In addition, we evaluated the cell viability of QDs capped with **Q-Gal** by the MTT (3-(4,5-dimethylthiazol-2-yl)-2,5-diphenyltetrazolium bromide) assay using Hep-G2 cells. The data showed that **Q-Gal** QDs were not toxic to cells even with a 10-fold increased concentration used for cellular imaging experiments (Supporting Information, Table S1). All these results suggest that **Q-Gal** QDs is a feasible photoluminogenic sensor for bioimaging of Hep-G2 cells expressing the galactose-specific ASGP-Rs. These observations also corroborate that our QD bioconjugates system conceived is well-suited for the target-specific (based on unique ligand−receptor recognitions) and switch-on (PL of QD bioconjugates restored after receptor−ligand binding) imaging of cancer cells.

■ CONCLUSIONS

In summary, we developed a novel strategy employing quinonyl glycosides functionalized QD bioconjugates as a "switch-on" PL biosensor for the biospecific imaging of Hep-G2 cells that express glycoprotein receptors. This unique sensing system, by taking advantage of the effective quenching ability of quinone for QDs and natural ligand−receptor recognitions (that recovers the signal), paves the way for the development of highly specific and low-background bioimaging materials for cancer cells. Our strategy might also provide valuable insights into the construction of photoluminogenic platforms for the probing of the universal ligand−receptor recognitions in nature.

dx.doi.org/10.1021/ac501463u | *Anal. Chem.* 2014, 86, 5502−5507

■ ASSOCIATED CONTENT

Supporting Information

Additional experimental section and figures. This material is available free of charge via the Internet at http://pubs.acs.org.

■ AUTHOR INFORMATION

Corresponding Authors

*E-mail: xphe@ecust.edu.cn. Fax: 86-21-64252758.
*E-mail: jli@mail.shcnc.ac.cn. Fax: 86-21-50800721.
*E-mail: ytlong@ecust.edu.cn. Fax: 86-21-64252339.

Author Contributions

The manuscript was written through contributions of all authors. All authors have given approval to the final version of the manuscript.

W.M. and H.-T.L. contributed equally to this work.

Notes

The authors declare no competing financial interest.

■ ACKNOWLEDGMENTS

This research was supported by the 973 Program (Grants 2013CB733700 and 2014CB748500), the National Natural Science Foundation of China (Grants 2115522, 21176076, 21202045, and 21305045), the Fundamental Research Funds for the Central Universities (Grant WJ1313004), the National Key Science & Technology Specific Projects (Grant 012ZX09301-001-004), and the Key Project of Shanghai Science and Technology Commission (Grant 13NM1400900).

■ REFERENCES

(1) May, L. T.; Leach, K.; Sexton, P. M.; Christopoulos, A. *Annu. Rev. Pharmacol. Toxicol.* **2007**, *47*, 1−51.
(2) Varki, A. *Glycobiology* **1993**, *3*, 97−130.
(3) Bertozzi, C. R.; Kiessling, L. L. *Science* **2001**, *291*, 2357−2364.
(4) Feizi, T.; Chai, W. *Nat. Rev. Mol. Cell Biol.* **2004**, *5*, 582−588.
(5) Seeberger, P. H. *Nature* **2004**, *437*, 1239−1239.
(6) Hart, G. W.; Copeland, R. J. *Cell* **2010**, *143*, 672−676.
(7) Robinson, A.; Fang, J.-M.; Chou, P.-T.; Liao, K.-W.; Chu, R.-M.; Lee, S.-J. *Chem. Bio. Chem.* **2005**, *6*, 1899−1905.
(8) Santra, S.; Kaittanis, C.; Santiesteban, O. J.; Perez, J. M. *J. Am. Chem. Soc.* **2011**, *133*, 16680−16688.
(9) Lee, M. H.; Han, J. H.; Kwon, P.-S.; Bhuniya, S.; Kim, J. Y.; Sessler, J. L.; Kang, C.; Kim, J. S. *J. Am. Chem. Soc.* **2012**, *134*, 1316−1322.
(10) Lee, M. H.; Kim, J. Y.; Han, J. H.; Bhuniya, S.; Sessler, J. L.; Kang, C.; Kim, J. S. *J. Am. Chem. Soc.* **2012**, *134*, 12668−12674.
(11) Liu, Y.; Zhou, S.; Tu, D.; Chen, Z.; Huang, M.; Zhu, H.; Ma, E.; Chen, X. *J. Am. Chem. Soc.* **2012**, *134*, 15083−15090.
(12) Gorityala, B. K.; Lu, Z.; Leow, M. L.; Ma, J.; Liu, X.-W. *J. Am. Chem. Soc.* **2012**, *134*, 15229−15232.
(13) Shinchi, H.; Wakao, M.; Nakagawa, S.; Mochizuki, E.; Kuwabata, S.; Suda, Y. *Chem.—Asian J.* **2012**, *7*, 2678−2682.
(14) Cao, X.; Cui, Y.; Levenson, R. M.; Chung, L. W. K.; Nie, S. *Nat. Biotechnol.* **2004**, *22*, 970−976.
(15) Palaniappan, K.; Xue, C.; Arumugam, G.; Hackney, S. A.; Liu, J. *Chem. Mater.* **2006**, *18*, 1275−1280.
(16) Ma, W.; Qin, L.-X.; Liu, F.-T.; Gu, Z.; Wang, J.; Pang, Z.-G.; James, T. D.; Long, Y.-T. *Sci. Rep.* **2013**, *3*, 1537.
(17) Medintz, I. L.; Stewart, M. H.; Trammell, S. A.; Susumu, K.; Delehanty, J. B.; Mei, B. C.; Melinger, J. S.; Blanco-Canosa, J. B.; Dawson, P. E.; Mattoussi, H. *Nat. Mater.* **2010**, *9*, 676−684.
(18) Qin, L.-X.; Ma, W.; Li, D.-W.; Li, Y.; Chen, X.; Kraatz, H.-B.; James, T. D.; Long, Y.-T. *Chem.—Eur. J.* **2011**, *17*, 5262−5271.
(19) Li, D.-W.; Qin, L.-X.; Li, Y.; Nia, R. P.; Long, Y.-T.; Chen, H. Y. *Chem. Commun.* **2011**, *47*, 8539−8541.
(20) Susumu, K.; Medintz, I. L.; Delehanty, J. B.; Boeneman, K.; Mattoussi, H. *J. Phys. Chem. C* **2010**, *114*, 13526−13531.
(21) Banerjee, S.; Kar, S.; Perez, J. M.; Santra, S. *J. Phys. Chem. C* **2009**, *113*, 9659−9663.
(22) Ji, X.; Palui, G.; Avellini, T.; Na, H. B.; Yi, C.; Knappenberger, K. L., Jr.; Mattoussi, H. *J. Am. Chem. Soc.* **2012**, *134*, 6006−6017.
(23) Palui, G.; Avellini, T.; Zhan, N.; Pan, F.; Gray, D.; Alabugin, I.; Mattoussi, H. *J. Am. Chem. Soc.* **2012**, *134*, 16370−16378.
(24) Zhan, N.; Palui, G.; Safi, M.; Ji, X.; Mattoussi, H. *J. Am. Chem. Soc.* **2013**, *135*, 13786−13795.
(25) He, X.-P.; Wang, X.-W.; Jin, X.-P.; Zhou, H.; Shi, X.-X.; Chen, G.-R.; Long, Y.-T. *J. Am. Chem. Soc.* **2011**, *133*, 3649−3657.
(26) Sabatino, M. A.; Galia, A.; Filardo, G.; Scialdone, O. *J. Appl. Electrochem.* **2009**, *39*, 2529−2533.
(27) Sabatino, M. A.; Filardo, G.; Galia, A.; Scialdone, O. *Electrochem. Commun.* **2007**, *9*, 1355−1358.
(28) Grogger, C.; Fattakhov, S. G.; Jouikov, V. V.; Shulaeva, M. M.; Reznik, V. S. *Electrochim. Acta* **2004**, *49*, 721−727.
(29) de la Fuente, J. M.; Barrientos, A. G.; Rojas, T. C.; Rojo, J.; Cañada, J.; Fernández, A.; Penadés, S. *Angew. Chem., Int. Ed.* **2001**, *40*, 2257−2261.
(30) Burda, C.; Green, T. C.; Link, S.; El-Sayed, M. A. *J. Phys. Chem. B* **1999**, *103*, 1783−1788.
(31) Williams, Y.; Sukhanova, A.; Nowostawska, M.; Davies, A. M.; Mitchell, S.; Oleinikov, V.; Gun'ko, Y.; Nabiev, I.; Kelleher, D.; Volkov, Y. *Small* **2009**, *22*, 2581−2588.
(32) He, L.; Zhang, Y. Z.; Tanoh, M.; Chen, G.-R.; Praly, J.-P.; Chrysina, E. D.; Tiraidis, C.; Kosmopoulou, M.; Leonidas, D. D.; Oikonomakos, N. G. *Eur. J. Org. Chem.* **2007**, *4*, 596−606.
(33) Lis, H.; Sharon, N. *Chem. Rev.* **1998**, *98*, 637−674.
(34) Braun, J. R.; Willnow, T. E.; Ishibashi, S.; Ashwell, G.; Herz, J. *J. Biol. Chem.* **1996**, *271*, 21160−21166.
(35) Yang, J.; Bo, X. C.; Ding, X. R.; Dai, J. M.; Zhang, M. L.; Wang, X. H.; Wang, S. Q. *J. Viral Hepatitis* **2006**, *13*, 158−165.
(36) Zhang, H.-L.; Wei, X.-L.; Zang, Y.; Cao, J.-Y.; Liu, S.; He, X.-P.; Chen, Q.; Long, Y.-T.; Li, J.; Chen, G.-R.; Chen, K. *Adv. Mater.* **2013**, *25*, 4097−4101.
(37) Li, Z.; Deng, S.-S.; Zang, Y.; Gu, Z.; He, X.-P.; Chen, G.-R.; Chen, K.; James, T. D.; Li, J.; Long, Y.-T. *Sci. Rep.* **2013**, *3*, 2293.
(38) Shi, D.-T.; Wei, X.-L.; Sheng, Y.; Zang, Y.; He, X.-P.; Xie, J.; Liu, G.; Tang, Y.; Li, J.; Chen, G.-R. *Sci. Rep.* **2014**, *4*, 4252.